



Employment of electrostriction phenomenon for label-free electrochemical immunosensing of tetracycline

Karolina Starzec^a, Cecilia Cristea^b, Mihaela Tertis^b, Bogdan Feier^b, Marcin Wieczorek^a, Paweł Kościelniak^a, Jolanta Kochana^{a,*}

^aJagiellonian University, Faculty of Chemistry, Department of Analytical Chemistry, Gronostajowa 2, 30-387 Kraków, Poland

^bIuliu Hațieganu University of Medicine and Pharmacy, Faculty of Pharmacy, Department of Analytical Chemistry, 4 Louis Pasteur St., 400349 Cluj-Napoca, Romania

ARTICLE INFO

Article history:

Received 28 March 2019

Received in revised form 7 October 2019

Accepted 7 October 2019

Available online 29 November 2019

Keywords:

Immunosensor

Antibacterial resistance

Tetracycline

SAM

Capacitive sensor

ABSTRACT

The presented work describes a simple label-free electrochemical immunosensor for the determination of tetracycline (TC). The functioning of the sensor was based on the electrostriction of an antibody-terminated thiol layer self-assembled on a gold electrode surface, serving as a dielectric membrane. The intensity of electrostriction was correlated with the amount of TC captured through an affinity reaction with its specific antibody, and was followed in the form of capacitance-potential curves. The process of the immunosensor construction was optimized using electrochemical impedance spectroscopy (EIS). The chemisorption time of the thiol, the duration of the TCAb immobilization and its concentration were optimized. The developed immunosensor exhibited a linear response in two concentration ranges: from 0.95 to 10 $\mu\text{mol L}^{-1}$ and from 10 to 140 $\mu\text{mol L}^{-1}$, with the mean sensitivity of 6.27 nF $\mu\text{mol}^{-1} \text{L}$ (88.67 nF $\mu\text{mol}^{-1} \text{L cm}^{-2}$) and 0.56 nF $\mu\text{mol}^{-1} \text{L}$ (7.84 nF $\mu\text{mol}^{-1} \text{L cm}^{-2}$), respectively. The limit of detection was evaluated as 28 nmol L^{-1} . The specificity of the proposed sensor toward other antibiotics, amoxicillin and ciprofloxacin, was examined. The immunosensor was successfully employed to quantify TC in a tablet form and in a matrix of river water.

© 2019 The Authors. Published by Elsevier B.V. This is an open access article under the CC BY-NC-ND license (<http://creativecommons.org/licenses/by-nc-nd/4.0/>).

1. Introduction

The development of new analytical methods designed for different compounds remains a continuous challenge for scientists. Simplicity, low cost and short time of analysis, high sensitivity and an appropriate limit of detection are the most desired characteristic parameters of new analytical procedures [1,2]. Electrochemical methods, particularly the ones using sensors, meet these requirements; however, most of them have one important limitation: they can be used only for the determination of electroactive compounds, as in voltammetry, or for the determination of ions which are able to cross membranes, which is the basis for potentiometric techniques [3,4]. Electrochemically inactive compounds can be determined using relatively complicated ion transfer voltammetry [5] or indirectly, e.g. employing molecularly imprinted electrodes [6]. Capacitive detection, based on electrostriction, creates an opportunity to easily circumvent mentioned limitation. Elec-

trostriction, which is a change in dimensions of the materials under the impact of an electric field, is specific to dielectrics [7]. In particular, it may be observed in monolayers – primarily, self-assembled monolayers (SAM). When a potential lower than 1 V is used for these layers, a strong electric field of 10^5 – 10^6 V cm^{-1} in intensity occurs [8,9]. Electrostatic forces alter the dimensions of the dielectric and the compression of the membrane and a decrease in thickness can be observed. Consequently, the membrane capacitance increases. Electrostriction can be observed in layers of long-chain organic compounds embedded onto the surface of a solid electrode which is immersed in an electrolyte solution. A self-assembled monolayer of thiols deposited onto a gold electrode can be considered a part of a capacitor, whose covers are the electrode surface and the electrolyte (analyte) solution [9,10]. Different interactions can occur between an analyte and the functional group of thiols exposed to the solution, like adsorption, a redox reaction, the formation of hydrogen/coordination bonds or an antigen-antibody reaction. These interactions influence the electrostriction and affect the measured signal – recorded as a capacitance-potential curve – proportional to the analyte concentration.

Immunosensors constitute a popular group of biosensors due to their unique selectivity and high sensitivity [11]. Their perfor-

* Corresponding author.

E-mail address: jolanta.kochana@uj.edu.pl (J. Kochana).

mance is based on the specific molecular recognition of antigens (usually the target analytes) by an antibody (Ab) on a transducer surface. The application of advanced electrochemistry combined with the capability of immunosensors allows the development of highly selective analytical devices designated for diverse target substances. Dozens of works pertain to immunosensing of specific biomarkers such as cancer and tumor biomarkers [12,13] or biomarkers of autoimmune diseases [14]. Some papers about immunosensors for the early screening of depression markers – the heat shock protein [15], or the detection of cardiac markers [16] have also been published. Furthermore, verification of the food quality [17] and environmental monitoring [18] using immunosensors have also been reported.

Antibiotics are among the most commonly used pharmaceuticals throughout the world. These drugs exhibit antibacterial properties and have been employed in the fight against bacterial infections in human and veterinary medicine. The widespread use of these drugs, combined with their misuse and overuse, has resulted in the ubiquitous presence of antibiotics in the human body, food products and animals, as well as in the environment [19]. Simultaneously, a global health problem of antibacterial resistance (ABR) has occurred. One of the crucial steps toward the control of antibiotics spreading over the world is the sensitive and accurate determination of antibiotic residues in every part of the environment, including environmental waters.

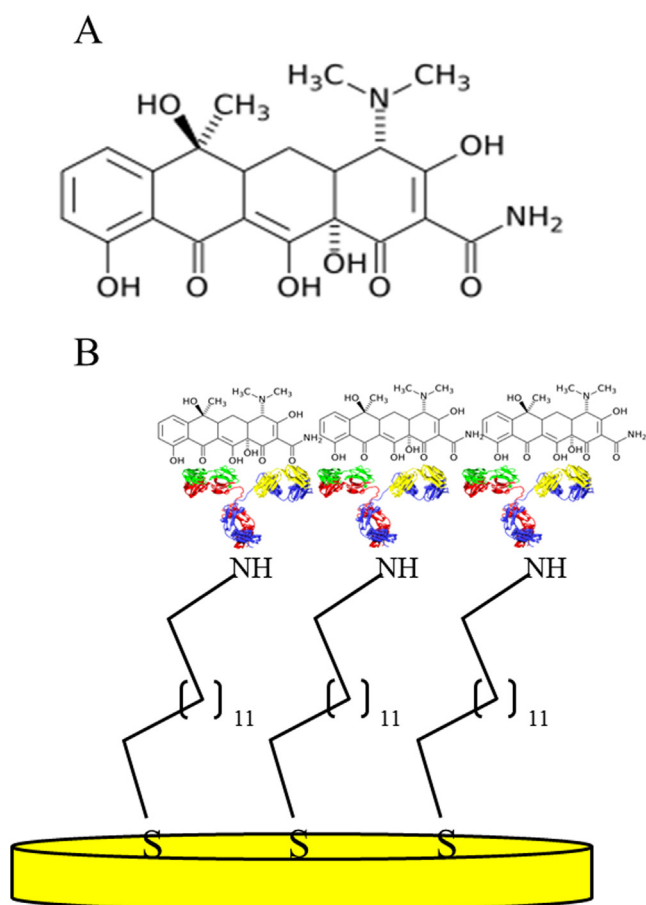
Tetracycline (TC) (see Scheme 1A) belongs to a group of antibiotics exhibiting broad-spectrum activity against many bacterial infections. Because of its availability, wide preventive effect and

low cost of manufacturing, it is probably the most used antibiotic in the animal breeding industry for protective and curative reasons [20]. TC is also often used in animal feed as growth agent [19,20]. The widespread and excessive use of the antibiotics has led to the ubiquitous presence of TC in the environment, especially in the environmental waters, contributing to the ABR processes. Tetracyclines constitute the class of antibiotics with the highest use in veterinary medicine, being used as first-line drugs in food animals, aquaculture, for treating exotic animals and honey bees. They also have non-antibiotic effects that are better documented for the second and third-generation [21]. For that reason, it is important to develop a rapid, sensitive and effective method for the determination of TC in a natural sample matrix.

Several methods for the determination of tetracycline residues have been published. Most often chromatographic methods have been reported [22,23]. Spectrophotometry [24] and the fluorescence technique [25] have also been proposed. These methods are usually complex, costly and time-consuming. In this context, the electrochemical methods seem to be a more attractive choice, because of their fairly rapid and cheap analysis, less expensive equipment and no need for special sample preparation. In the literature, a few types of electrochemical immunosensors and sensors for the quantification of TC have been described, including immunosensors based on the anti-TC antibody (TCAb) [26–28] and sensors modified with metal nanoparticles [29–31]. Some electrochemical sensors are also based on molecularly imprinted polymers [32], graphene [33] or reduced graphene oxide [34].

The present work is focused on the development and application of a new capacitive immunosensor for TC determination. The active layer of the immunosensor is composed of a self-assembled monolayer of 11-amino-1-undecane thiol (SAM) whose amino group allows the formation of an amide bond with the carboxyl group of the TCAb. A schematic illustration of the developed immunosensor (TCAb/SAM/AuE) is presented in Scheme 1B. The elastic thiols monolayer terminated with the antibiotic antibody, serving as a dielectric membrane, underwent electrostriction [7]. Its intensity was proportional to the concentration of the analyte solution and was recorded and followed in the form of capacitance-potential curves [8–10]. The capacitive measurements were carried out using the capacitance-to-frequency conversion method [8,35]. The production of the immunosensor was optimized, taking into account the SAM chemisorption time, the time of TCAb immobilization and its concentration. The progress of optimization was studied using electrochemical impedance spectroscopy (EIS). The immunosensor was evaluated with respect to: linear range, sensitivity, limit of detection, limit of quantification and reproducibility. Moreover, the selectivity of the proposed sensor toward TC in the presence of amoxicillin and ciprofloxacin was examined. For verification purposes, the proposed immunosensor was successfully used for tetracycline determination in an antibiotic tablet available on the Polish pharmaceutical market, and for analysis of the Vistula river water spiked with the analyte without any special sample pre-treatment.

To the best of our knowledge, there has been no study to date on an immunosensor based on the electrostriction phenomenon quantified by capacitance-potential characteristics for antibiotics detection. So far, the capacitance-to-frequency conversion method has been used as a detection method in the electrochemical determination of simple inorganic ions [9,36]. In our work, for the first time this detection approach has been employed in the field of immunosensors. Moreover, in this work, electrostriction phenomenon, which is based on the changes in dimensions of the dielectric compounds occurring as elastic strains when an electric field is applied, was combined with antibodies, obtaining an extremely selective method for antibiotics detection.



Scheme 1. Structural formula of tetracycline (A) and schematic illustration of the developed capacitive immunosensor (B).

2. Experimental

2.1. Chemicals and solutions

The following reagents were used in the performed research: tetracycline hydrochloride $C_{22}H_{24}N_2O_8 \cdot HCl$, (Sigma-Aldrich, USA); 11-amino-1-undecanethiol hydrochloride $HSCH_2(CH_2)_9CH_2NH_2 \cdot HCl$, 99% (Sigma-Aldrich, USA); anti-TC polyclonal antibody 9.98 mg mL^{-1} (ThermoFisher Scientific, USA); diamond suspension with grain size $0.5 \mu\text{m}$ (Leco, USA); diamond suspension with grain size $0.1 \mu\text{m}$ (Struers, United Kingdom); OP-Nat wool polishing cloth, 200 mm (8"), (Struers, United Kingdom); potassium hexacyanoferrate $K_4[Fe(CN)_6]$, >99% (POCh, Poland); potassium hexacyanoferrate $K_3[Fe(CN)_6]$, >99% (POCh, Poland); sodium dihydrogen phosphate NaH_2PO_4 , >99.5% (POCh, Poland); disodium hydrogen phosphate dihydrate $Na_2HPO_4 \cdot 2H_2O$, >99% (POCh, Poland); potassium hydroxide KOH, 99% (Centro-chem, Poland); potassium chloride KCl, 99.5% (POCh, Poland); potassium nitrate KNO_3 , 99% (Chempur, Poland); ethanol C_2H_6O , 99.8% (POCh, Poland); sulfuric acid H_2SO_4 , 95–97% (Merck, Germany); hydrogen peroxide H_2O_2 , 30% (Chempur, Poland); buffer solutions (Elmetron, Poland) of pH = 4.00, 6.00 and 8.00 for the pH electrode calibration; sodium sulphite Na_2SO_3 (Elmetron, Poland) for preparing 0% solution for oxygen sensors calibration; concentrated sulfuric acid H_2SO_4 98% (Merck, Germany), potassium dichromate $K_2Cr_2O_7$ (Chempur, Poland), potassium chromium sulfate $KCr(SO_4)_2$ (Chempur, Poland), silver sulfate Ag_2SO_4 (POCh, Poland) and mercury(II) sulfate $HgSO_4$ (POCh, Poland) for Chemical Oxygen Demand determination; formic acid $HCOOH$ (Sigma-Aldrich, USA); acetonitrile CH_3CN , gradient grade for liquid chromatography (Merck, Germany), antibiotic tablet Tetracyclinum TZF 250 mg (Polfa, Poland). Ultrapure water ($18.2 \text{ M}\Omega$) after reversed osmosis (HLP, Hydrolab, Poland) was used throughout the research.

In this work, the following solutions were used: piranha solution prepared by mixing concentrated H_2SO_4 and 30% H_2O_2 in a volume ratio 3:1; 1 mmol L^{-1} thiol solution prepared by dissolving 1.2 mg thiol in 5 mL 99.8% ethanol; 0.1, 0.2 and 0.5 mg mL^{-1} TCAB solutions prepared by dilution of 1, 2 and $5 \mu\text{L}$ (from 9.98 mg mL^{-1}) in $99 \mu\text{L}$ phosphate buffer solution (PBS) (20 mmol L^{-1} ; pH 7.4), respectively; 1 mmol L^{-1} TC stock solution prepared by dissolving 4.8090 mg of solid tetracycline in 10 mL PBS at a concentration of 20 mmol L^{-1} and pH 7.4.

2.2. Apparatus and measurement procedures

The majority of electrochemical experiments were performed using Autolab PGSTAT30 and Autolab PGSTAT302N (Metrohm, Eco Chemie Netherlands), both being equipped with an EIS module, operated using Nova 1.10.4 software. Preliminary electrochemical characterization and optimization of the immunosensor construction were performed by electrochemical impedance spectroscopy and cyclic voltammetry (CV). The experiments were carried out in a solution of 5 mmol L^{-1} $[Fe(CN)_6]^{3-/4-}$ prepared in a phosphate buffer (PBS) (20 mmol L^{-1} ; pH 7.4). CV experiments were performed in a potential range of $-0.4 - 0.8 \text{ V}$ at a scan rate of 0.05 V s^{-1} using portable potentiostat/galvanostat Palmsens3 (Palmsens BV, the Netherlands). The frequency window for impedance measurements was from 10 kHz to 100 kHz , at open circuit potential and an amplitude of 10 mV . For EIS measurements, screen-printed electrodes (SPE) (DropSens, Spain) with an integrated three-electrode cell based on a gold working electrode with a 4 mm diameter, a silver reference and a carbon counter electrode were used. A solid gold working electrode, AuE (3 mm diameter), was used in the construction of the capacitive immunosensor.

Dielectric capacitance experiments were performed using the capacitance meter CMTR-243 (KSP Elektronika Laboratoryjna, Poland), composed of a galvanostat, a capacitance meter and A/D and D/A converters [35]. Capacitance measurements were conducted using the capacitance-to-frequency conversion method. They were carried out in a conventional three-electrode system with the following electrodes placed in the quartz cell: the working electrode (WE) – gold electrode with 3 mm diameter (MTM Anko M10X1, Poland), covered with a thiol monolayer with an immobilized TCAB; the reference electrode (RE) – silver chloride electrode ($Ag/AgCl$, saturated $KCl/2 \text{ mol L}^{-1} KNO_3$) with a double coat (MTM Anko M6, Poland); and the auxiliary electrode (AE) – platinum wire placed in a teflon holder. The capacitance measurements were performed in the potential range of $0.2 - 0.6 \text{ V}$ at a scan rate of 0.05 V s^{-1} and a potential step of 5 mV . The experiments were carried out in a 5 mL electrochemical cell, first in a supporting electrolyte, PBS at a concentration of 20 mmol L^{-1} at pH 7.4, and then in solutions of increasing tetracycline concentration. For each solution, ten measurement cycles were performed to stabilize the course of the capacitive-potential curve. It was observed that after every eighth scan the curves overlapped, and therefore for analytical purposes every ninth measurement cycle was used.

The Vistula river samples were examined at the sampling site using the portable multifunction meter for field and laboratory work CX-701 (Elmetron, Poland), using an IJ44A (Elmetron, Poland) pH electrode, an ECF-1t (Elmetron, Poland) conductivity cell of $K = 0.45 \text{ cm}^{-1}$ with metal electrodes and equipped with a built-in temperature sensor, and a COG-1t (Elmetron, Poland) oxygen sensor.

For comparative purposes, TC was determined using a LCMS-8050 mass spectrometer coupled to a LC-30AD Liquid Chromatograph Nexera2, equipped with a SIL-30AC Autosampler Nexera2 (all Shimadzu, Japan). The column was Ascentis Express C18 ($5 \text{ cm} \times 2.1 \text{ mm}$, $2.7 \mu\text{m}$, Supelco, USA) maintained at 25°C . The eluents used were as follows: ultrapure water with 0.1% formic acid (A), acetonitrile with 0.1% formic acid (B). The flow rate was 1 mL/min . The injection volume was $2 \mu\text{L}$ and the analyte was eluted over a 3 min binary gradient with a starting composition percentage of 95/5 (A/B). The LCMS-8050 is a three-quadrupole mass spectrometer with a heated electrospray ionization source. TC was detected in positive MRM mode and ion for $410.10 \pm 0.01 (m/z)$ was used as analytical signal. The retention time of TC was 1.25 min .

2.3. Construction of the capacitive immunosensor

The immunosensor production is an only two-stage process and requires a simple thiol and an antibody. It was prepared by the chemisorption of 11-amino-1-undecanethiol onto the gold electrode surface followed by the immobilization of the TCAB through applying a drop of TCAB solution onto the electrode surface. The most important step, before assembling the thiols monolayer, was the appropriate preparation of the electrode surface by removing impurities adsorbed on the gold and smoothing the surface roughness.

2.3.1. Cleaning of the gold electrodes

The surface of the gold electrodes was cleaned electrochemically and mechanically. First, the electrodes were cleaned electrochemically to remove the previous thiol monolayer by performing twenty voltammetric cycles in a 0.5 mol L^{-1} potassium hydroxide solution in the potential range of $-0.2 - 1.2 \text{ V}$ at a scan rate of 0.02 V s^{-1} . Then, electrodes were polished manually by drawing '8' shapes on two polishing cloths, for four minutes on each cloth, soaked in diamond suspension with a grain size of 0.5 and $0.1 \mu\text{m}$, respectively. After each polishing step, the electrodes were rinsed

with water. Finally, the electrodes were immersed in piranha solution for 30 s. Purification in piranha solution was followed by cyclic voltammetry experiments using a Fe(II)/Fe(III) redox probe ($5 \text{ mmol L}^{-1} [\text{Fe}(\text{CN})_6]^{3-/4-}$ in a 20 mmol L^{-1} supporting electrolyte solution, PBS at pH 7.4) in the potential range of $-0.4 - 0.8 \text{ V}$. The potential difference between a pair of well-defined redox peaks of Fe(II)/Fe(III) conversion (ΔE_p) was used as a measure of the electrochemical cleanliness of the electrode surface. In theory, according to the Nernst equation, for a one-electron redox process, ΔE_p should be 0.058 V [37]. In practice, a potential difference in the range of $0.08 - 0.10 \text{ V}$ was assumed to be satisfactory.

2.3.2. Electrode modification

After the cleaning process, the electrode surfaces were modified in two major steps. The first one was the chemisorption of 11-amino-1-undecanethiol by immersing the electrodes in a thiol solution of concentration 1 mmol L^{-1} . After that, to verify that the electrodes were covered by a thiol monolayer, EIS measurements were performed in a $5 \text{ mmol L}^{-1} [\text{Fe}(\text{CN})_6]^{3-/4-}$ solution. The next step of electrode modification was the immobilization of the TCAb by dropping $25 \mu\text{L}$ of TCAb solution onto the surface of the electrode. Then, the quality of the antibody immobilization was verified by EIS measurements in a redox couple Fe(II)/Fe(III). And so, finally, the finished immunosensor for TC determination was ready: it had a flexible thiol monolayer with an immobilized antibody, which undergoes electrostriction under the influence of an electric field. Particular stages of the immunosensor construction are shown in Scheme 2.

2.4. Samples preparation

The pharmaceutical sample of TC tablets was prepared as follows: after removing the color coating of the antibiotic tablet, the white tablet (core) was crushed in an agate mortar; next, the whole powdered tablet was transferred quantitatively to a volumetric flask containing around 200 mL of distilled water and sonicated for 10 min . The solution was filled up to 1.0 L with distilled water and a stock solution with a predicted concentration of 250 mg L^{-1} TC was obtained.

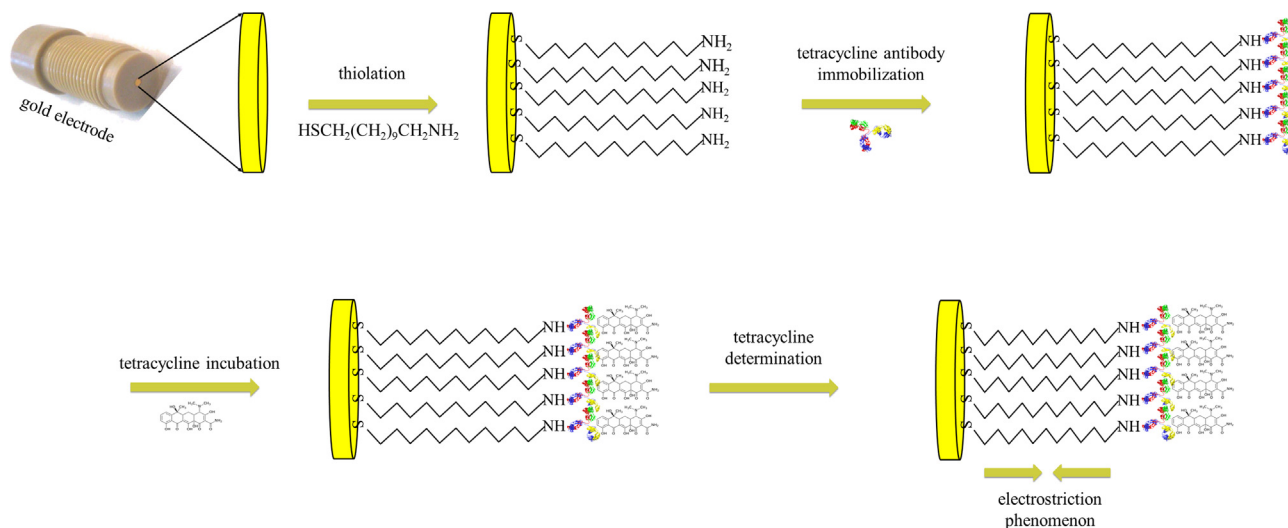
The water sample from the Vistula River was taken with a 0.5 L sample water scoop made of polypropylene at the place of a large flow rate and about 0.5 m below the surface. At the sampling site, the following parameters were measured: water temperature

($21.2 \text{ }^\circ\text{C}$), pH (7.36 ± 0.12), conductivity ($1.32 \pm 0.5 \text{ mS cm}^{-1}$) and oxygen percentage ($52.8 \pm 4.2\%$). The samples were poured into 250 mL polypropylene containers, closed without air and then transported to the laboratory in a portable refrigerator at $5 \text{ }^\circ\text{C}$. Immediately after bringing the samples to the lab, the water was filtered through filter paper and a Buchner funnel. Chemical Oxygen Demand (COD-Cr(VI)) of $28.5 \pm 0.6 \text{ mg L}^{-1}$ was obtained according to the ISO Standard 6060:1989. All tests were performed three times in the same conditions and average values with confidence interval ($2\alpha = 0.05$) are presented above. To prepare the sample of spiked Vistula river water, 2.4 mg of tetracycline hydrochloride was weighed and transferred quantitatively to a volumetric flask with a small volume of Vistula water. After dissolving the tetracycline, the flask was filled up to 100 mL with Vistula river water and mixed. A spiked sample of mineral water "Nałęczowianka" was prepared in the same way as the river water sample. The prepared solutions of the antibiotic tablets, spiked river and mineral waters were adequate diluted with PBS or ultra-pure water for capacitive or LC-MS measurements, respectively.

3. Results and discussion

3.1. Optimization of the immunosensor construction

In order to create an immunosensor characterized by good analytical parameters, optimization studies were carried out. It was decided to optimize three parameters which were considered important for the functioning of a capacitive immunosensor: thiolation time, time of TCAb immobilization and its concentration. The optimization studies were performed utilizing gold screen-printed electrodes (Au SPE), and the results were finally validated on solid gold electrodes (AuE), which were used in the construction of the immunosensor. Each stage involved in the immunosensor development was evaluated by EIS. An equivalent electrical circuit (Randles circuit) was applied and the parameters were evaluated by fitting the model with experimental data using NOVA1.10.4 software. Thus, for the unmodified screen-printed gold electrode, a $[R_s(Q1[R_{ct}W])]$ circuit type was proposed (Fig. 1A). Different components were included in this circuit, namely, the electrolyte solution resistance (R_s), the resistance of electron (charge) transfer at the solution-electrode interface (R_{ct}), the Warburg impedance (W) and a constant phase element ($CPE1 = Q1$). It may be noted



Scheme 2. Schematic diagram of stepwise immunosensor construction.

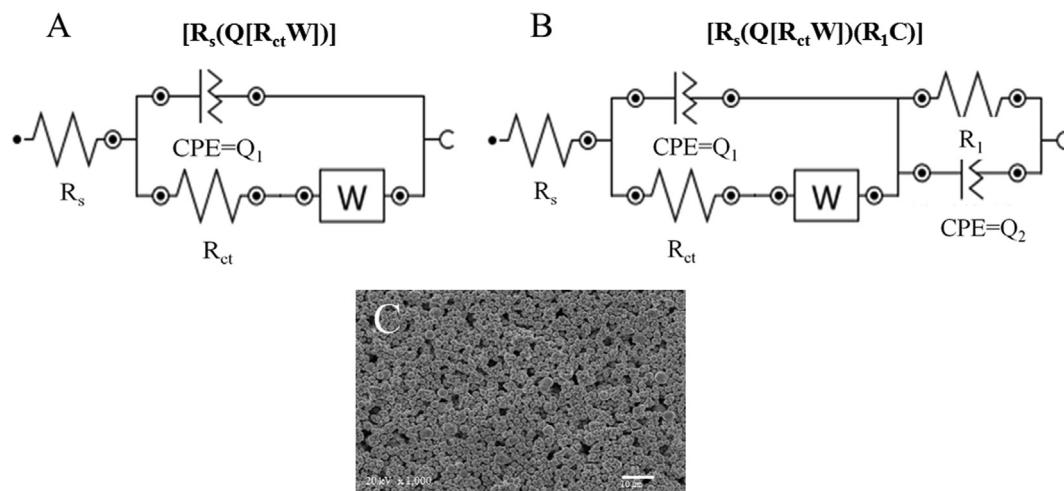


Fig. 1. The equivalent electric circuits used for fitting the EIS data obtained for the unmodified Au SPE (A), the Au SPEs after different modifications (functionalization with thiol; antibody immobilization; and tetracycline capturing) (B), SEM image of the unmodified Au SPE (C).

that the capacitance was replaced by a constant phase element ($CPE = Q$) determined by the porosity of the working electrode, as was observed from a SEM image recorded for this surface (Fig. 1C). After modification of the electrode, the equivalent circuit was changed, and a resistance and a CPE were introduced. Thus, the new circuit was $[R_s(Q_1[R_{ct}W])(R_1Q_2)]$, as shown in Fig. 1B. The need to introduce new components was related to changes on the surface of the gold electrode, namely the immobilization of the different organic and biological compounds (thiol, TCAB and TC). The second CPE element could have been inserted due to high variability in the structure, composition and thickness of the film deposited on the electrode, in which case the conductivity of the film will vary across the electrode [38–40]. This type of circuit is utilized for the theoretical representation of a double-layer capacitance model and is usually suitable for describing the mechanism that takes place at the surface of biosensors based on composite films [41,42].

The optimization experiments were carried out for three independent Au SPEs. Each step of the sensor preparation was investigated using EIS. Any change in the electrode conductivity, confirming its successful modification, was revealed through variation of the R_{ct} values. The results of EIS experiments, obtained for exemplary Au SPE during the optimization protocol, are shown in Fig. 2 and the values for all fitted parameters corresponding to the Nyquist graphs are presented in Table S1 (see Supplementary information). The mean R_{ct} values calculated for three experiments carried out on each step of the optimization procedure are shown in Table S2. These results were taken into account in further discussion. Student's t -test was used to verify if the difference between the mean R_{ct} values, obtained for different optimization parameters, were statistically significant at $\alpha = 0.05$. Earlier, the F-test was employed to confirm that no significant differences occurred between obtained variances.

3.1.1. Optimization of the thiolation time

Firstly, the thiolation time was optimized (see Fig. 2B). Based on the continuous increase in the R_{ct} value with thiolation time, 24 h was selected as the optimal duration for this stage of the immunosensor preparation. An increase in the R_{ct} value from 102 Ω registered for the bare screen-printed Au electrode, to 878 Ω after 24 h of thiolation was noted (see Table S2 in Supplementary information).

3.1.2. Optimization of the tetracycline antibody immobilization

In order to ensure the best immobilization of the antibodies, different times for the immobilization of TCAB and antibody solutions of different concentrations were examined. The results obtained by EIS for exemplary Au SPE are presented in Fig. 2C and D. A noticeable increase in the R_{ct} values, from 1008 Ω to 1736 Ω , obtained for 2 and 4 h of immobilization, respectively, was noticed at this stage of optimization (see Table S2). Based on the t -test carried out, it was stated that further extension of the incubation time did not result in a significant increase in the R_{ct} values, so 4 h was chosen as the optimal time for antibody immobilization. The sensitivity of the immunosensor is strictly dependent on the antibody concentration. Therefore, three different concentrations of TCAB solutions were tested. As shown in Fig. 2D, no significant changes were revealed, which was confirmed using the t -test for the mean R_{ct} values. Therefore, a concentration of 0.1 mg mL⁻¹ was selected for further experiments.

3.1.3. Preparation of TCAB/SAM/AuE

In the next stage of research, using the results of the optimization studies, a capacitive immunosensor based on a solid gold electrode, AuE, was constructed. EIS and CV experiments, repeated for three independent electrodes, were conducted to electrochemically characterize the electrode after each step of the immunosensor preparation. Based on the EIS measurements, overlaid Nyquist representations were obtained. After modeling the data using the NOVA10.10.4 software options, the same equivalent electric circuits were proposed as for the screen-printed gold electrode. Exemplary Nyquist plots and the values for all fitted parameters corresponding to these graphs are presented in Fig. 3A and Table S3, respectively. It can be seen that each step of the immunosensor construction caused an increase in the R_{ct} value. The same was observed for the other two electrodes. Thus, for a bare electrode, a R_{ct} of 411 Ω ($SD = 13 \Omega$) was obtained, while after 24 h incubation with 1 mmol L⁻¹ thiol solution, an increase in the R_{ct} value to 3380 Ω ($SD = 147 \Omega$) was noted, confirming the successful modification of the electrode. The incubation of the SAM/AuE in 0.1 mg L⁻¹ TCAB solution for 4 h caused a dramatic increase in the R_{ct} to 10,118 Ω ($SD = 563 \Omega$), indicating an increase in the coverage of the conductive surface of the electrode. Another significant rise in the R_{ct} value was observed after the incubation of the target analyte, tetracycline, this time being more than double compared with the previous step (23,150 Ω , $SD = 881 \Omega$). The results of analogous

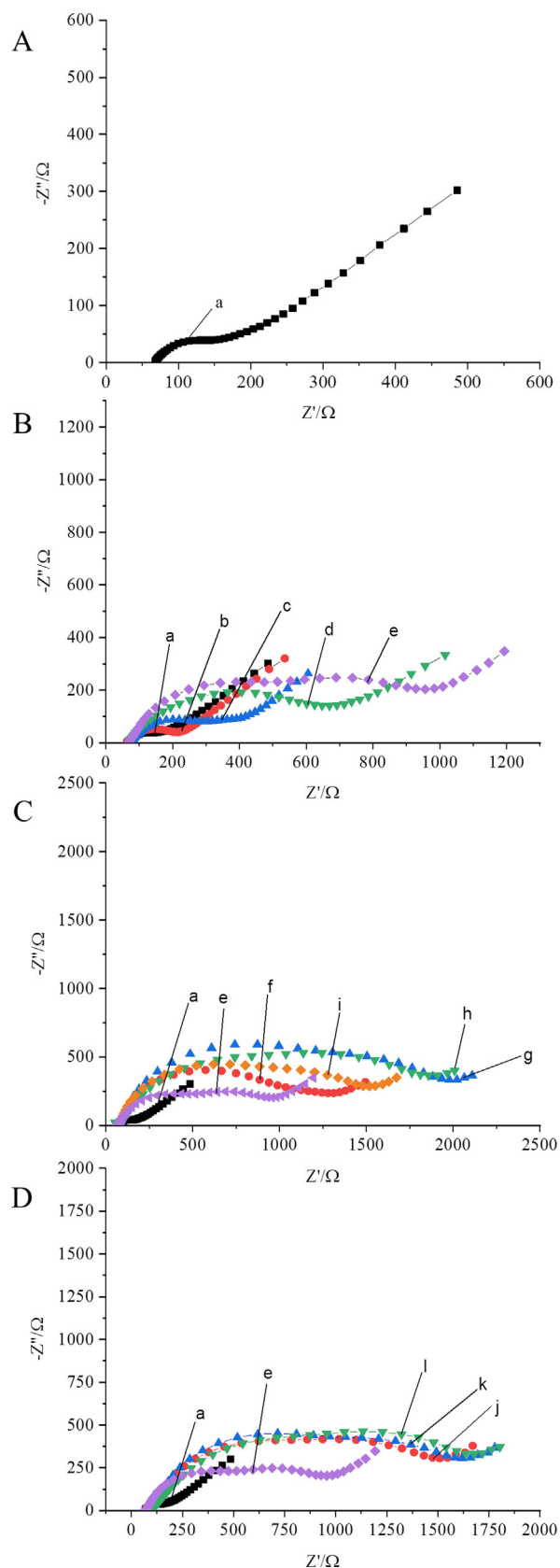


Fig. 2. Nyquist diagrams for the bare Au SPE (a) (A), the Au SPEs recorded after different thiolation times: 2, 6, 12 and 24 h (b–e) (B), after different TCab immobilization times: 2, 4, 6 and 16 h (f–i) (C), and registered for different TCab concentrations: 0.1, 0.2 and 0.5 mg mL⁻¹ (j and k) (D); measurements were performed in 20 mmol L⁻¹ PBS, pH 7.4, containing 5 mmol L⁻¹ [Fe(CN)₆]^{3-/4-}.

CV experiments recorded for one of the tested AuE are shown in Fig. 3B. It can be seen that the highest peak intensities, both for the oxidation and reduction processes, were obtained for the cleaned and unmodified electrodes (black curve a). Modification of the AuE with thiol (red curve b), tetracycline antibody (blue curve c), as well as tetracycline incubation (green curve d), blocked the electroactive surface of the electrode making the undergoing of the redox processes incrementally more difficult. It can be seen that the decrease in the current peak intensities was dependent on the modification step. The same relationships were observed for the other two electrodes. Comparing the average results of CV and EIS tests it was concluded that there was a good correlation between the observations made for both methods, confirming the correctness of the proposed immunosensor construction method. Then, the developed immunosensor was employed for the capacitive determination of TC.

3.2. Analytical characteristic of the developed capacitive immunosensor

The analytical pattern of each TCab/SAM/AuE was recorded as a characteristic hysteresis loop, showing changes in the capacitance as a function of the applied potential. The example of the recorded relationships is shown in Fig. 4A. Some variation of the capacitive-potential curves recorded for different sensors was observed [8–10]. This phenomenon may result from the non-ideal smoothness of the gold surface after the electrode preparing process and, consequently, unrepeatable assembling of thiols on the gold electrode surface. During the research, it was noticed that capacitance characteristics moved down along the capacitance axis with increasing concentration of analyte, as is presented in Fig. 4A. The analytical signal – the value of the capacitance correlated to the particular analyte concentration – was read for the WE potential exhibiting the highest sensor sensitivity. The choice of the optimal readout potential was based on a comparison of relationships of the capacitance versus the TC concentration recorded, for the given sensor, for different potential values. In Fig. 4B, the graphs obtained for different WE potentials, corresponding to the curves shown in Fig. 4A, are presented. It can be seen that the highest sensor sensitivity was noted for a potential of 0.4 V. Therefore, for this particular sensor, the capacitance values registered at that potential were taken as the analytical signal.

The use of the capacitive detection required the selection of an adequate calibration approach [9,36]. The specificity of capacitive measurements, resulting from the uniqueness of the capacitive patterns acquired for different sensors, necessitated the implementation of the whole measurement procedure using the same sensor in a solution of increasing analyte concentrations. Additionally, it should be taken into account that the signal measured for the supporting electrolyte was not usually present on the linear calibration graph with the remaining measurement points (see Fig. 4B). Bearing in mind the above, a modified standard addition calibration method, known as the signal increment standard addition method (SISAM), was employed [36]. Briefly, the first standard addition was added to the measuring cell containing the supporting electrolyte and the analytical signal was recorded, R1 (see Fig. 5A). Then, a sample solution with an unknown concentration of analyte and known volume was introduced into the cell and the next analytical signal was measured, R2. Afterwards, analytical signals R3–R6 were registered for four subsequent standard additions. Based on the recorded signals (R2–R6), a calibration graph was plotted and the unknown sample concentration was obtained by extrapolation of the calibration plot to the first standard solution signal, R1. An exemplary calibration curve obtained using SISAM for determination of TC in 0.95 μmol L⁻¹ synthetic sample is shown in Fig. 5B.

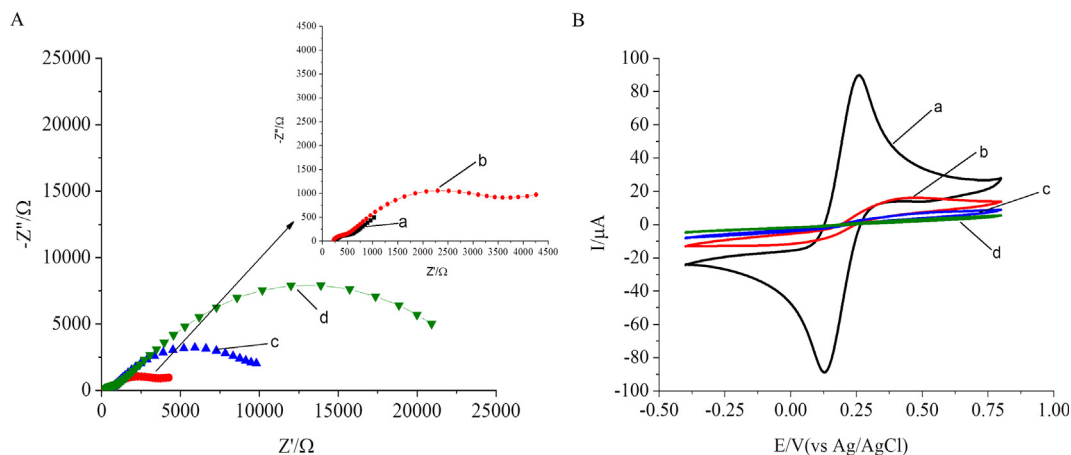


Fig. 3. Nyquist diagrams for the bare AuE (a), and the AuE during immunosensor preparation after each modification step including thiolation (b), tetracycline antibody immobilization (c), and tetracycline incubation (d) (A); cyclic voltammograms (a–d) corresponding to the same modification steps (B); EIS and CV curves were recorded in 20 mmol L⁻¹ PBS, pH 7.4, containing 5 mmol L⁻¹ [Fe(CN)₆]^{3-/4-}.

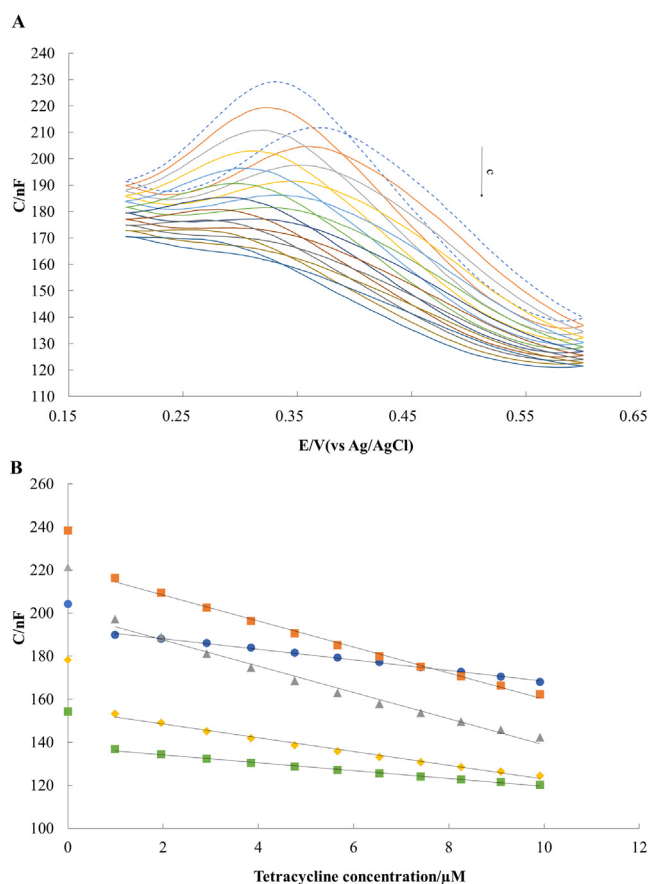


Fig. 4. Example of capacitance-potential curves recorded for ten consecutive additions of the tetracycline standard solution in a concentration range from 0.95 to 10.0 $\mu\text{mol L}^{-1}$ (A), and the corresponding calibration graphs plotted for five different potentials (for 0.2 V: $y = -2.41x + 192.66$, $R^2 = 0.996$; for 0.3 V: $y = -6.17x + 221.38$, $R^2 = 0.996$; for 0.4 V: $y = -6.36x + 201.65$, $R^2 = 0.985$; for 0.5 V: $y = -3.33x + 155.8$, $R^2 = 0.989$; for 0.6 V: $y = -1.92x + 138.47$, $R^2 = 0.990$) (B).

The developed immunosensor displayed a linear electrochemical response toward tetracycline within two linear ranges: from 0.95 to 10 $\mu\text{mol L}^{-1}$ and from 10 to 140 $\mu\text{mol L}^{-1}$. The following linear relationships of the capacitance as a function of concentration (C – c) were obtained, as mean values for five sensors for each concentration range:

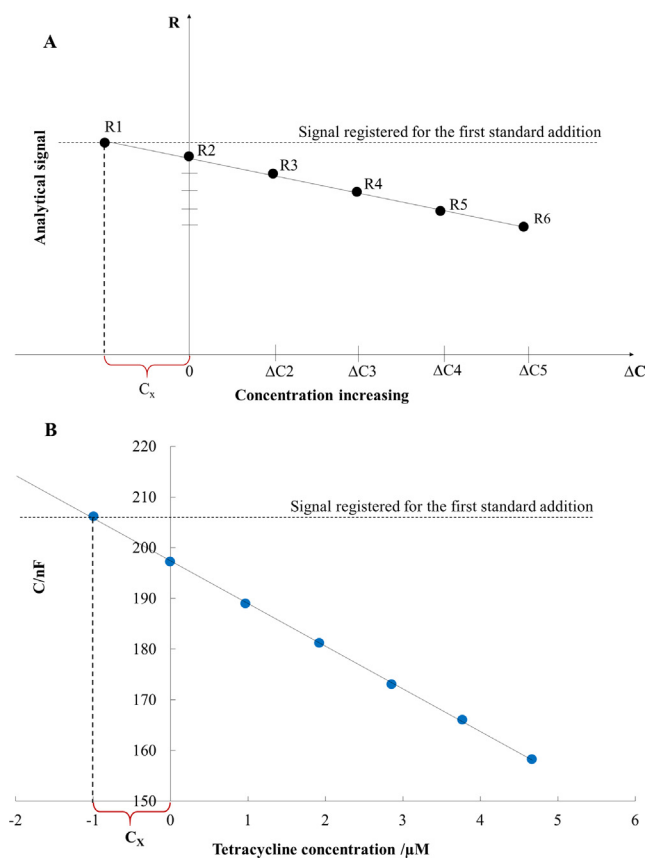


Fig. 5. General approach of the used calibration method (SISAM) (A), and an exemplary calibration graph ($y = -6.43x + 201.65$, $R^2 = 0.995$) illustrating the application of SISAM obtained for analysis of the 0.95 $\mu\text{mol L}^{-1}$ synthetic sample (B).

up to 10 $\mu\text{mol L}^{-1}$ C [nF] = 6.27 (± 1.10) [nF μmol^{-1} L] $\cdot c$ [$\mu\text{mol} \cdot \text{L}^{-1}$] + 237.3 (± 6.6) [nF],
up to 140 $\mu\text{mol L}^{-1}$ C [nF] = 0.56 (± 0.05) [nF μmol^{-1} L] $\cdot c$ [$\mu\text{mol L}^{-1}$] + 189.5 (± 2.5) [nF],

(standard deviations were calculated based on the law of propagation of uncertainty). The limit of detection, LOD = 28 nmol L⁻¹, was estimated based on the formula $3s/a$, where s is the standard deviation of signals recorded for a 0.95 $\mu\text{mol L}^{-1}$ tetracycline solu-

Table 1
Comparison of the analytical characteristics of the electrochemical immunosensors and the sensors designed for tetracycline determination.

Electrode*	Detection**	Linear range [$\mu\text{mol L}^{-1}$]	LOD [$\mu\text{mol L}^{-1}$]	Reference
TCAb-MNPs-CS/AuE	DPV	0.0002–0.0023	0.0001	[23]
TCAb/mAg/AuNPs/GCE	SWASV	0.00002–0.1125	0.000017	[24]
TCAb/TC-BSA/PtGN/AuE	LSV	0.0001–0.2250	0.000014	[25]
MIOPPy-AuNP/SPCE	DPV	1–20	0.65	[26]
PtNPs/C/GCE	CV	9.99–44.01	4.28	[27]
RuSiNPs/Nafion/GCE	ECL	1.00–100.00	0.23	[28]
GR-SPCEs	DPV	1–20 and 20–100	0.08	[30]
p-Mel@ERGO/GC	DPV	5–225	2.2	[31]
CB-PS/GCE	DPV	5–120	1.15	[41]
Fe/Zn-MMT/GCE	DPV	0.30–52.00	0.10	[42]
4-ABA/ProtG/HRP/SPdCEs	AM	0.006–0.385	0.0019	[43]
ProtG-MBs/HRP/SPCE	AM	0.028–1.522	0.0088	[44]
TCAb/SAM/AuE	Capacitive	1–10 and 10–140	0.028	This work

* 4-ABA/ProtG/HRP/SPdCEs – protein G immobilized onto a 4-aminobenzoic acid and horseradish peroxidase for the enzymatic labeling on the screen-printed dual carbon electrodes, CB-PS/GCE – a homogeneous thin film of potato starch and carbon black deposited on glassy carbon electrode, TCAb-MNPs-CS/AuE – gold electrode-modified carboxyl- Fe_3O_4 nanoparticle by chitosan as linker with anti-tetracycline antibody immobilized on the modified electrode surface, TCAb/mAg/AuNPs/GCE – biotin-labeled tetracycline antibody conjugates with bovine serum albumin coimmobilized on a glassy carbon electrode modified with gold nanoparticles, TCAb/TC-BSA/PtGN/AuE – platinum/graphene nanosheets as the labeling of tetracycline-bovine serum albumin conjugates for tetracycline antibody immobilization, MIOPPy-AuNP/SPCE – screen-printed carbon electrode modified with molecularly imprinted overoxidized polypyrrole and gold nanoparticles, PtNPs/C/GCE – platinum nanoparticles supported on carbon on glassy carbon electrode, RuSiNPs/Nafion/GCE – ruthenium-doped silica nanoparticles and Nafion film on glassy carbon electrode, GR-SPCE – graphene screen-printed carbon electrode, p-Mel@ERGO/GC – a polymelamine film on electrochemically reduced graphene oxide on a glassy carbon electrode, ProtG-MBs/HRP/SPCE – protein G-functionalized magnetic beads on screen-printed carbon electrode and horseradish peroxidase for the enzymatic labeling, Fe/Zn-MMT/GCE – iron/zinc cation-exchanged montmorillonite catalyst on glassy carbon electrode, TCAb/SAM/AuE – tetracycline antibody bounded with self-assembled monolayer (SAM) of 11-amino-1-undecanethiol on the solid gold electrode;

** AM – amperometry, DPV – differential pulse voltammetry, SWASV – square wave anodic stripping voltammetry, LSV – linear sweep voltammetry, CV – cyclic voltammetry, ECL – electrochemiluminescence.

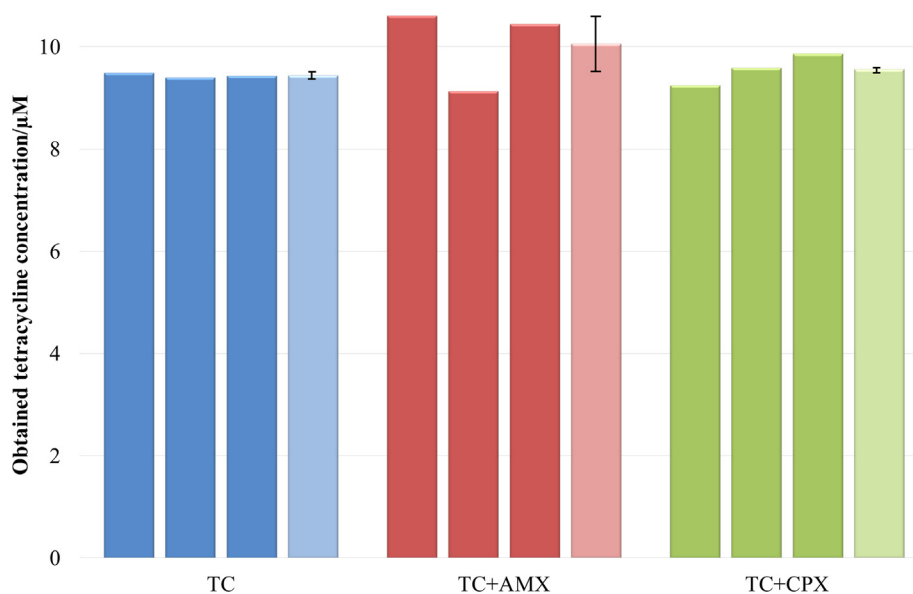


Fig. 6. The results of specificity studies obtained for the $9.52 \mu\text{mol L}^{-1}$ tetracycline solution (blue), mixtures of tetracycline and amoxicillin solutions (red), and tetracycline and ciprofloxacin solutions (green), all at a concentration of $9.52 \mu\text{mol L}^{-1}$; results obtained for three independent repetitions (deep colors) and acquired mean values (light colors) with bars showing relative errors. (For interpretation of the references to color in this figure legend, the reader is referred to the web version of this article.)

tion ($n = 6$), and a is the sensor sensitivity [43]. The reproducibility was verified in a $9.5 \mu\text{mol L}^{-1}$ tetracycline solution, for three independently constructed immunosensors, giving a RSD (relative standard deviation) value of 0.29%. The developed TCAb/SAMs/AuE immunosensor was compared to other electrochemical immunosensors and sensors produced for tetracycline determination with respect to linear range and limit of detection (Table 1). The best analytical parameters were declared for the immunosensors based on TCAb, where the measuring technique was square wave anodic stripping voltammetry [27] and linear sweep voltammetry [28]. However, it can be seen that the proposed TCAb/SAMs/AuE exhibited good analytical parameters. The limit of detection obtained for the developed sensor is lower than the one reported

for most of the other sensors [29–31,33,34,44,45]. A few sensors and immunosensors described in the literature [26–28,46,47] exhibited a lower LOD value, but at the same time the linear ranges reported for these sensors were significantly narrower. Moreover, the proposed SAMs/TCAb/AuE was characterized by almost the widest linear range.

3.3. Specificity studies

The crucial challenge in the development of new immunosensors is achieving good specificity. The presence of substances that can influence the signal obtained for an analyte often turns out to be a problem because of the interference effects. Therefore, it

Table 2

Results of the tetracycline determination in synthetic and natural samples.

Sample	Concentration of tetracycline (μM)		Mean	RE%	RSD%	Recovery %
	Expected	Found				
Synthetic sample I	0.95	0.95 0.99 0.94	0.96	1.1	1.6	101.1
Synthetic sample II	9.52	9.49 9.40 9.44	9.44	−0.8	0.3	99.2
Synthetic sample III	18.85	16.60 18.35 20.73	18.56	−1.5	6.4	98.5
Vistula river water	6.63	7.36 6.94 6.97	7.09	6.9	1.9	106.9
Antibiotic tablets	9.52	10.90 9.53 9.09	9.84	3.4	5.5	103.4

was necessary to verify the substrate specificity of the developed TCab/SAMs/AuE. For this purpose, two antibiotics, amoxicillin and ciprofloxacin, were taken into account as potential interferents; they can be encountered in waste waters, for example in the waste from hospitals. The influence of interfering substances on the analytical results obtained for a $9.52 \mu\text{mol L}^{-1}$ TC solution was tested using the same concentration of potential interferent in each case. The results of specificity studies are presented in Fig. 6. As can be seen, neither amoxicillin nor ciprofloxacin considerably changed the capacitive signal obtained for tetracycline. The accuracy of the sensor in the determination of tetracycline in the presence of amoxicillin and ciprofloxacin expressed as relative error ($n = 3$) was 5.68% and 0.76%, respectively, whereas the precision given as the RSD value was 4.65% and 1.86%, respectively.

3.4. Verification of immunosensor functioning. Synthetic and natural samples analyses

To verify the usefulness of the constructed immunosensor, analyses of synthetic and natural samples were carried out. The synthetic solutions were examined at three tetracycline concentration levels with triple repetitions at each level. An antibiotic tablet and environmental water from the Vistula River were chosen. The capacitive measurements performed in the Vistula water did not generate an analytical signal, so it was assumed that it did not contain the antibiotic, and, the river water sample was spiked with analyte solution. The results of the performed determinations are presented in Table 2. It can be seen that the proposed capacitive immunosensor exhibited good accuracy, since the obtained relative error (RE%) values were lower than 8.0%. The precision of the proposed approach was satisfactory because the relative standard deviation (RSD%) did not exceed 6.5%. Therefore, it can be concluded that the developed TCab/SAM/AuE immunosensor combined with an adequate calibration method could provide valuable analytical results.

To confirm the trueness of the results obtained using the proposed immunosensor, LC-MS was employed as a reference method. TC was determined from an antibiotic tablet, as well as from mineral and river water samples spiked with the analyte. Each sample was analyzed three times. As shown in Table 3, the concentration values obtained for proposed electrochemical and chromatographic methods are in good agreement.

4. Conclusion

A novel immunological label-free electrochemical method for TC quantification using electrostriction of a self-assembled mono-

Table 3

Comparison of the determination results obtained for samples containing tetracycline with the use of TCab/SAMs/AuE and LC-MS method.

Sample	Concentration of tetracycline (μM) ^a	
	TCab/SAMs/AuE	HPLC-MS
Mineral water	2.85 ± 0.15	2.88 ± 0.08
Vistula river water	1.05 ± 0.09	1.14 ± 0.08
Antibiotic tablets	2.64 ± 0.19	2.73 ± 0.31

^a $C_{\text{found}} \pm (SD/\sqrt{n}) t_{2n-1}$; $n = 3$, $\alpha = 0.05$.

layer of thiol, chemisorbed on a gold electrode, terminated with a TCab has been presented. The developed TCab/SAM/AuE immunosensor exhibited good analytical characteristics in relation to tetracycline, especially regarding the low value of the LOD and the wide linear range. A great advantage of the developed immunosensor is the simplicity of its preparation. The production is an only two-stage process and requires a simple thiol-containing linker and an antibody. However, the construction of the proposed capacitive sensor takes longer compared to other reported immunosensors, ca. 28 h and several hours, respectively [26–28,47,48]. Furthermore, it should be noted that the preparation of the electrodes exhibiting repeatable capacitance-potential characteristics can be problematic, and strongly depends on the quality of the gold electrode surface. Nevertheless, even for an immunosensor whose capacitive characteristics differ from others, the proposed procedure for processing measurement data ensures that accurate and precise results can be obtained.

Further research could be focused on the implementation of the developed analytical procedure using disposable screen-printed gold electrodes. There are reports about such immunosensors that have been designed for TC quantification [47,48]. The use of disposable screen-printed sensors will make the proposed methodology an attractive tool for on-site analysis.

The matrix of the developed sensor has the potential to be used in the preparation of other immunosensors, as every antibody can be used to create an immunoelectrode. In this way, the proposed methodology can be used to determine other electrochemically inactive analytes, provided that the appropriate antibody is available.

Declaration of Competing Interest

The authors declared that there is no conflict of interest.

Acknowledgments

The study was supported by Polish National Science Centre, Project 2013/11/B/ST4/00864.

Appendix A. Supplementary material

Supplementary data to this article can be found online at <https://doi.org/10.1016/j.bioelechem.2019.107405>.

References

- [1] Z. Yu, Y. Tang, G. Cai, R. Ren, D. Tang, Paper electrode-based flexible pressure sensor for point-of-care immunoassay with Gan, *Anal. Chem.* 91 (2019) 1222–1226, <https://doi.org/10.1021/acs.analchem.8b04635>.
- [2] R. Ren, G. Cai, Z. Yu, Y. Zeng, D. Tang, Metal-polydopamine framework: an innovative signal-generation tag for colorimetric immunoassay, *Anal. Chem.* 90 (2018) 11099–11105, <https://doi.org/10.1021/acs.analchem.8b03538>.
- [3] R. Zeng, Z. Luo, L. Su, L. Zhang, D. Tang, R. Niessner, D. Knopp, Palindromic molecular beacon based z-scheme biocl-aucds photoelectrochemical biodection, *Anal. Chem.* 91 (2019) 2447–2454, <https://doi.org/10.1021/acs.analchem.8b05265>.
- [4] M. Puiu, C. Bala, Peptide-based biosensors: From self-assembled interfaces to molecular probes in electrochemical assays, *Bioelectrochemistry* 120 (2018) 66–75, <https://doi.org/10.1016/j.bioelechem.2017.11.009>.
- [5] S.R. Puri, J. Kim, Kinetics of antimicrobial drug ion transfer at a water/oil interface studied by nanopipet voltammetry, *Anal. Chem.* 91 (3) (2019) 1873–1879, <https://doi.org/10.1021/acs.analchem.8b03593>.
- [6] D. Capoferri, M. Del Carlo, N. Ntshongontshi, E.I. Iwuoha, M. Sergi, F. Di Ottavio, D. Campagnone, MIP-MEPS based sensing strategy for the selective assay of dimethoate. Application to wheat flour samples, *Talanta* 174 (2017) 599–604, <https://doi.org/10.1016/j.talanta.2017.06.062>.
- [7] A.V. Babakov, L.N. Ermishkin, E.A. Lieberman, Influence of electric field on the capacity of phospholipid membranes, *Nature* 210 (1966) 953–955, <https://doi.org/10.1038/210953b0>.
- [8] J. Kochana, K. Starzec, M. Wiecezorek, P. Knihnicki, M. Góra, A. Rokicińska, P. Kościelniak, P. Kuśtrowski, Study on self-assembled monolayers of functionalized thiol on gold electrode forming capacitive sensor for chromium(VI) determination, *J. Solid State Electrochem.* 23 (2019) 1463–1472, <https://doi.org/10.1007/s10008-019-04236-2>.
- [9] M. Wiecezorek, J. Kochana, P. Knihnicki, K. Wapiennik, P. Kościelniak, Novel electroanalytical method based on the electrostriction phenomenon and its application to determination of Cr(VI) by the flow injection technique, *Talanta* 166 (2017) 383–390, <https://doi.org/10.1016/j.talanta.2016.01.031>.
- [10] J. Kilian, S. Kalinowski, J. Kochana, P. Knihnicki, A new capacitive sensor based on electrostriction phenomenon. Application for determination of ionic surfactants, *Procedia Eng.* 47 (2012) 1338–1341, <https://doi.org/10.1016/j.proeng.2012.09.403>.
- [11] A. Pollap, J. Kochana, Electrochemical Immunosensors for antibiotic detection, *Biosensors* 9 (2019) 61, <https://doi.org/10.3390/bios9020061>.
- [12] Y. Zeng, J. Bao, Y. Zhao, D. Huo, M. Chen, Y. Qi, M. Yang, H. Fa, C. Hou, A sandwich-type electrochemical immunoassay for ultrasensitive detection of non-small cell lung cancer biomarker CYFRA21-1, *Bioelectrochemistry* 120 (2018) 183–189, <https://doi.org/10.1016/j.bioelechem.2017.11.003>.
- [13] A.K. Yagati, M.-H. Lee, J. Min, Electrochemical immunosensor for highly sensitive and quantitative detection of tumor necrosis factor- α in human serum, *Bioelectrochemistry* 122 (2018) 93–102, <https://doi.org/10.1016/j.bioelechem.2018.03.007>.
- [14] X. Zhang, A. Zambrano, Z.T. Lin, Y. Xing, J. Rippey, T. Wu, Immunosensors for biomarker detection in autoimmune diseases, *Arch. Immunol. Ther. Ex.* 65 (2017) 111–121, <https://doi.org/10.1007/s00005-016-0419-5>.
- [15] B. Sun, J. Cai, W. Li, X. Gou, Y. Gou, D. Li, F. Hu, A novel electrochemical immunosensor based on PG for early screening of depression markers-heat shock protein 70, *Biosens. Bioelectron.* 111 (2018) 34–40, <https://doi.org/10.1016/j.bios.2018.03.049>.
- [16] S.K. Tuteja, R. Chen, M. Kukkar, C.K. Song, R. Mutreja, S. Singh, A.K. Paul, H. Lee, K.H. Kim, A. Deep, C.R. Suri, A label-free electrochemical immunosensor for the detection of cardiac marker using graphene quantum dots (GQDs), *Biosens. Bioelectron.* 86 (2016) 548–556, <https://doi.org/10.1016/j.bios.2016.07.052>.
- [17] L. Zong, Y. Jiao, X. Guo, Ch. Zhu, L. Gao, Y. Han, L. Li, Ch. Zhang, Z. Liu, J. Liu, Q. Ju, H.-D. Yu, W. Huang, Paper-based fluorescent immunoassay for highly sensitive and selective detection of norfloxacin in milk at picogram level, *Talanta* 195 (2019) 333–338, <https://doi.org/10.1016/j.talanta.2018.11.073>.
- [18] P. Fruhmann, A. Sanchis, L. Mayerhuber, T. Vanka, C. Kleber, J.P. Salvador, M.P. Marco, Immunoassay and amperometric biosensor approaches for the detection of deltamethrin in seawater, *Anal. Bioanal. Chem.* 410 (2018) 5923–5930, <https://doi.org/10.1007/s00216-018-1209-1>.
- [19] E.D. Brown, G.D. Wright, Antibacterial drug discovery in the resistance era, *Nature* 529 (2016) 336–343, <https://doi.org/10.1038/nature17042>.
- [20] M. Pérez-Rodríguez, R.G. Pellerano, L. Pezza, H.R. Pezza, An overview of the main foodstuff sample preparation technologies for tetracycline residue determination, *Talanta* 182 (2018) 1–21, <https://doi.org/10.1016/j.talanta.2018.01.058>.
- [21] J.R.E. del Castillo, Tetracyclines, in: S. Giguère, J.F. Prescott, P.M. Dowling (Eds.), *Antimicrobial Therapy in Veterinary Medicine*, Wiley Blackwell, 2013.
- [22] A. Grande-Martínez, D. Moreno-González, F.J. Arrebola-Liebanas, A. Garrido-Frenich, A.M. García-Campaña, Optimization of a modified QuEChERS method for the determination of tetracyclines in fish muscle by UHPLC–MS/MS, *J. Pharmaceut. Biomed.* 155 (2018) 27–32, <https://doi.org/10.1016/j.jpba.2018.03.029>.
- [23] M.R. Jadhav, A. Pudale, P. Raut, S. Utture, T.P. Ahammed Shabeer, K. Banerjee, A unified approach for high-throughput quantitative analysis of the residues of multi-class veterinary drugs and pesticides in bovine milk using LC-MS/MS and GC-MS/MS, *Food Chem.* 272 (2019) 292–305, <https://doi.org/10.1016/j.foodchem.2018.08.033>.
- [24] M. Pérez-Rodríguez, H.R. Pezza, L. Pezza, Simple and clean determination of tetracyclines by flow injection analysis, *Spectrochim. Acta. A* 153 (2016) 386–392, <https://doi.org/10.1016/j.saa.2015.08.048>.
- [25] H. Li, L. Zhao, Y. Xu, T. Zhou, H. Liu, N. Huang, J. Ding, Y. Li, L. Ding, Single-hole hollow molecularly imprinted polymer embedded carbon dot for fast detection of tetracycline in honey, *Talanta* 185 (2018) 542–549, <https://doi.org/10.1016/j.talanta.2018.04.024>.
- [26] X. Liu, S. Zheng, Y. Hu, Z. Li, F. Luo, Z. He, Electrochemical immunosensor based on the chitosan-magnetic nanoparticles for detection of tetracycline, *Food Anal. Method.* 9 (2016) 2972–2978, <https://doi.org/10.1007/s12161-016-0480-z>.
- [27] B. Liu, B. Zhang, G. Chen, D. Tang, Biotin-avidin-conjugated metal sulfide nanoclusters for simultaneous electrochemical immunoassay of tetracycline and chloramphenicol, *Microchim. Acta* 181 (2014) 257–262, <https://doi.org/10.1007/s00604-013-1096-2>.
- [28] X. Que, X. Chen, L. Fu, W. Lai, J. Zhuang, G. Chen, D. Tang, Platinum-catalyzed hydrogen evolution reaction for sensitive electrochemical immunoassay of tetracycline residues, *J. Electroanal. Chem.* 704 (2013) 111–117, <https://doi.org/10.1016/j.jelechem.2013.06.023>.
- [29] L. Devkota, L.T. Nguyen, T.T. Vu, B. Piro, Electrochemical determination of tetracycline using AuNP-coated molecularly imprinted overoxidized polypyrrole sensing interface, *Electrochim. Acta* 270 (2018) 535–542, <https://doi.org/10.1016/j.electacta.2018.03.104>.
- [30] R.T. Kushikawa, M.R. Silva, A.C.D. Angelo, M.F.S. Teixeira, Construction of an electrochemical sensing platform based on platinum nanoparticles supported on carbon for tetracycline determination, *Sensor. Actuat. B-Chem.* 228 (2016) 207–213, <https://doi.org/10.1016/j.snb.2016.01.009>.
- [31] X. Chen, L. Zhao, X. Tian, S. Lian, Z. Huang, X. Chen, A novel electrochemiluminescence tetracyclines sensor based on a Ru(bpy)₃²⁺-doped silica nanoparticles/Nafion film modified electrode, *Talanta* 129 (2014) 26–31, <https://doi.org/10.1016/j.talanta.2014.04.054>.
- [32] M. Bougrini, A. Florea, C. Cristea, R. Sandulescu, F. Vocanson, A. Errachid, B. Bouchikhi, N. El Bari, N. Jaffrezic-Renault, Development of a novel sensitive molecularly imprinted polymer sensor based on electropolymerization of a microporous-metal-organic framework for tetracycline detection in honey, *Food Control* 59 (2016) 424–429, <https://doi.org/10.1016/j.foodcont.2015.06.002>.
- [33] H. Filik, A.A. Avan, S. Aydar, D. Ozyurt, B. Demirata, Determination of tetracycline on the surface of a high-performance graphene modified screen-printed carbon electrode in milk and honey samples, *Cur. Nanosci.* 12 (2016) 527–533, <https://doi.org/10.2174/1573413712666151214222808>.
- [34] S. Kesavan, D.R. Kumar, Y.R. Lee, J.-J. Shim, Determination of tetracycline in the presence of major interference in human urine samples using polymelamine/electrochemically reduced graphene oxide modified electrode, *Sensor. Actuat. B-Chem.* 241 (2017) 455–465, <https://doi.org/10.1016/j.snb.2016.10.091>.
- [35] S. Kalinowski, Z. Figaszewski, A four-electrode system for measurement of bilayer lipid membrane capacitance, *Meas. Sci. Technol.* 6 (1995) 1043–1049, <https://doi.org/10.1088/0957-0233/6/7/028>.
- [36] M. Wiecezorek, M. Madej, K. Starzec, P. Knihnicki, A. Telk, J. Kochana, P. Kościelniak, Flow manifold for chemical H-point standard addition method implemented to electrochemical analysis based on the capacitance measurements, *Talanta* 186 (2018) 183–191, <https://doi.org/10.1016/j.talanta.2018.03.098>.
- [37] L.M. Fischer, M. Tenje, A.R. Heiskanen, N. Masuda, J. Castillo Leon, A. Bentien, J. Emnéus, M.H. Jakobsen, A. Boisen, Gold cleaning methods for electrochemical detection applications, *Microelectron. Eng.* 86 (2009) 1282–1285, <https://doi.org/10.1016/j.mee.2008.11.045>.
- [38] Z. Kerner, T. Pajkossy, On the origin of capacitance dispersion of rough electrodes, *Electrochim. Acta* 46 (2000) 207–211, [https://doi.org/10.1016/S0013-4686\(00\)00574-0](https://doi.org/10.1016/S0013-4686(00)00574-0).
- [39] J. Bisquert, G. García-Belmonte, P.R. Bueno, E. Longo, L. Bulhões, Impedance of constant phase element (CPE)-blocked diffusion in film electrodes, *J. Electroanal. Chem.* 452 (1998) 229–234, [https://doi.org/10.1016/S0022-0728\(98\)00115-6](https://doi.org/10.1016/S0022-0728(98)00115-6).
- [40] J.-B. Jorcin, M.E. Orazem, N. Pebere, B. Tribollet, CPE analysis by local electrochemical impedance spectroscopy, *Electrochim. Acta* 51 (2006) 1473–1479, <https://doi.org/10.1016/j.electacta.2005.02.128>.
- [41] T.T.N. Lien, T.D. Lam, V.T.H. An, T.V. Hoang, D.T. Quang, D.Q. Khieu, T. Tsukahara, Y.H. Lee, J.S. Kim, Multi-wall carbon nanotubes (MWCNTs)-doped polypyrrole DNA biosensor for label-free detection of genetically modified organisms by QCM and EIS, *Talanta* 80 (2010) 1164–1169, <https://doi.org/10.1016/j.talanta.2009.09.002>.
- [42] A. Baraket, M. Lee, N. Zine, M. Sigaud, J. Bausells, A. Errachid, A fully integrated electrochemical biosensor platform fabrication process for cytokines detection, *Biosens. Bioelectron.* 93 (2017) 170–175, <https://doi.org/10.1016/j.bios.2016.09.023>.

- [43] A. Pollap, P. Knihnicki, P. Kuśtrowski, J. Kozak, M. Gołda-Cępa, A. Kotarba, J. Kochana, Sensitive voltammetric amoxicillin sensor based on TiO₂ sol modified by CMK-3-type mesoporous carbon and gold nanoparticles, *Electroanal.* 30 (2018) 2386–2396, <https://doi.org/10.1002/elan.201800203>.
- [44] K.P. Delgado, P.A. Raymundo-Pereira, A.M. Campos, O.N. Jr Oliveira, B.C. Janegitz, Ultralow cost electrochemical sensor made of potato starch and carbon black nanoballs to detect tetracycline in waters and milk, *Electroanal.* 30 (2018) 2153–2159, <https://doi.org/10.1002/elan.201800294>.
- [45] T. Gan, Z. Shi, J. Sun, Y. Liu, Simple and novel electrochemical sensor for the determination of tetracycline based on iron/zinc cations-exchanged montmorillonite catalyst, *Talanta* 121 (2014) 187–193, <https://doi.org/10.1016/j.talanta.2014.01.002>.
- [46] R. Rapini, G. Marrazza, Electrochemical aptasensors for contaminants detection in food and environment: recent advances, *Bioelectrochemistry* 118 (2017) 47–61, <https://doi.org/10.1016/j.bioelechem.2017.07.004>.
- [47] F. Conzuelo, M. Gamella, S. Campuzano, A.J. Reviejo, J.M. Pingarrón, Disposable amperometric magneto-immunosensor for direct detection of tetracyclines antibiotics residues in milk, *Anal. Chim. Acta* 737 (2012) 29–36, <https://doi.org/10.1016/j.aca.2012.05.051>.
- [48] F. Conzuelo, S. Campuzano, M. Gamella, D.G. Pinacho, A.J. Reviejo, M.P. Marco, J.M. Pingarrón, Integrated disposable electrochemical immunosensors for the simultaneous determination of sulfonamide and tetracycline antibiotics residues in milk, *Biosens. Bioelectron.* 50 (2013) 100–105, <https://doi.org/10.1016/j.bios.2013.06.019>.